Supplement of Atmos. Chem. Phys., 23, 3595–3607, 2023
https://doi.org/10.5194/acp-23-3595-2023-supplement

Atmospheric Chemistry and Physics
Open Access

Supplement of

Elucidating ozone and $PM_{2.5}$ pollution in the Fenwei Plain reveals the co-benefits of controlling precursor gas emissions in winter haze

Chunshui Lin et al.

Correspondence to: Ru-Jin Huang (rujin.huang@ieecas.cn)

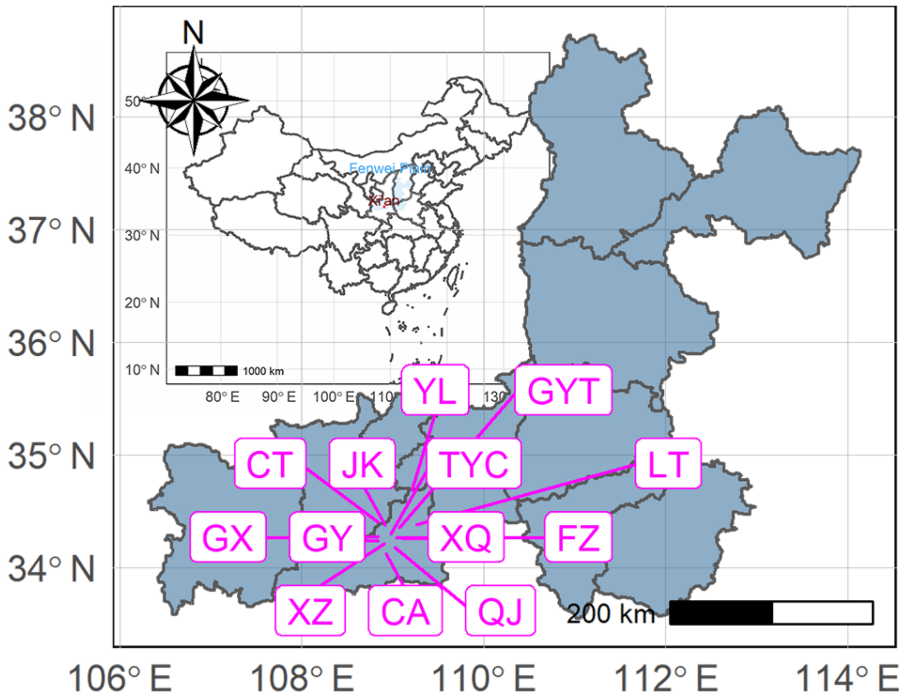

Figure S1. The 13 monitoring sites in urban Xi'an, the largest city in the Fenwei Plain. All 13 sampling sites are classified as urban sites within Xi'an city. GY: GaoYa kaiguanchang; XQ: XingQing community; FZ: FanZhi city; XZ: XiaoZhai; TYC: shirenmin TiYuChang; GX: GaoXin new district; JK: JingKai district; CA: ChangAn district; YL: YanLiang district; LT: LinTong district; CT: CaoTan district; QJ: QuJiang wehuachanyejituan; GYT: GuangYunTan.

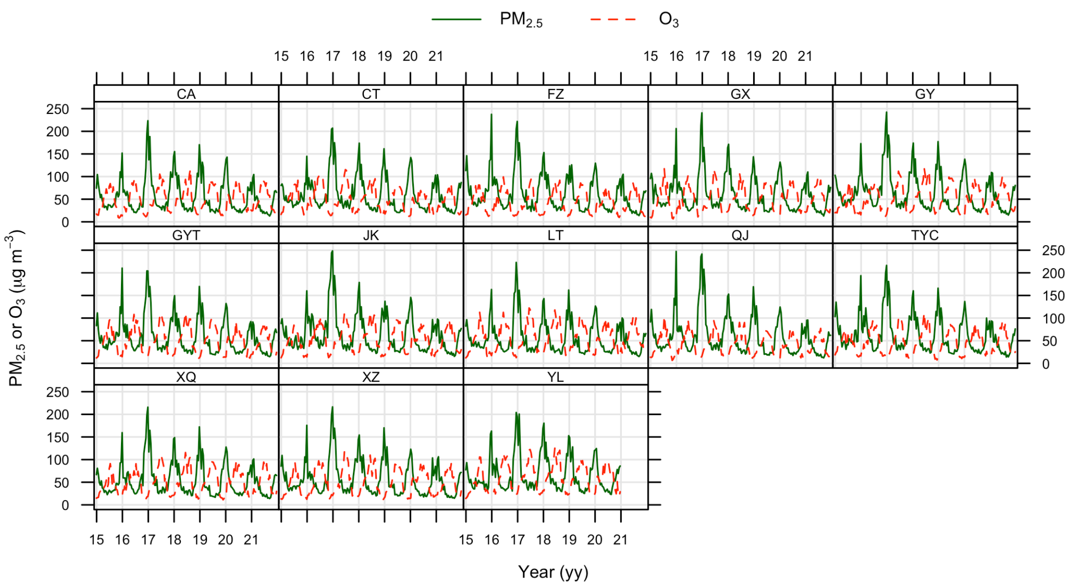

Figure S2. Time series of $PM_{2.5}$ and O_3 at the 13 sampling sites from 2015 to 2021. The abbreviation for the sampling site is the same as in Figure S1. Data were averaged at 2 weeks for clarity reasons.

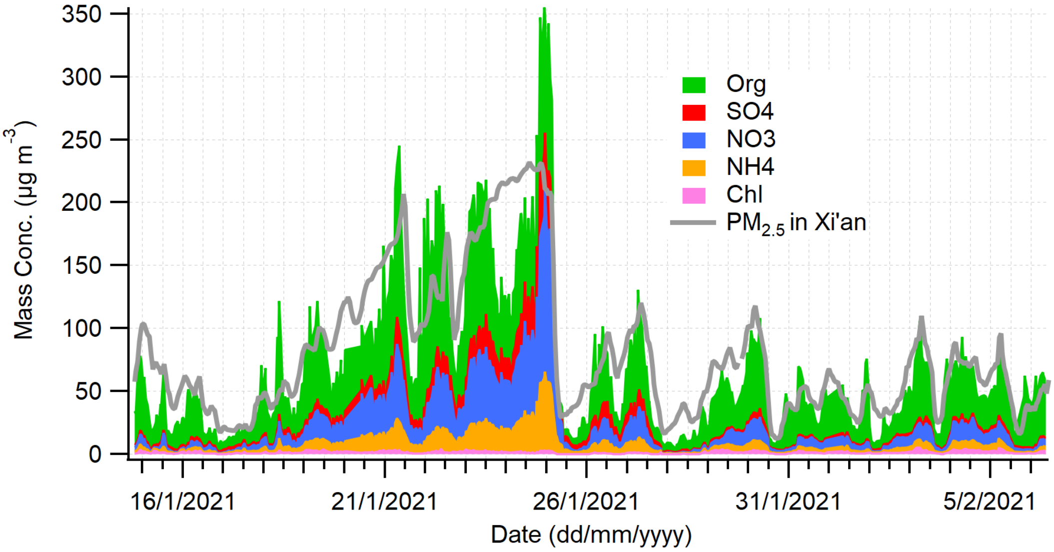

Figure S3. Time series of the NR-PM$_{2.5}$ species and the mean PM$_{2.5}$ concentrations from January 14 to February 6, 2021.

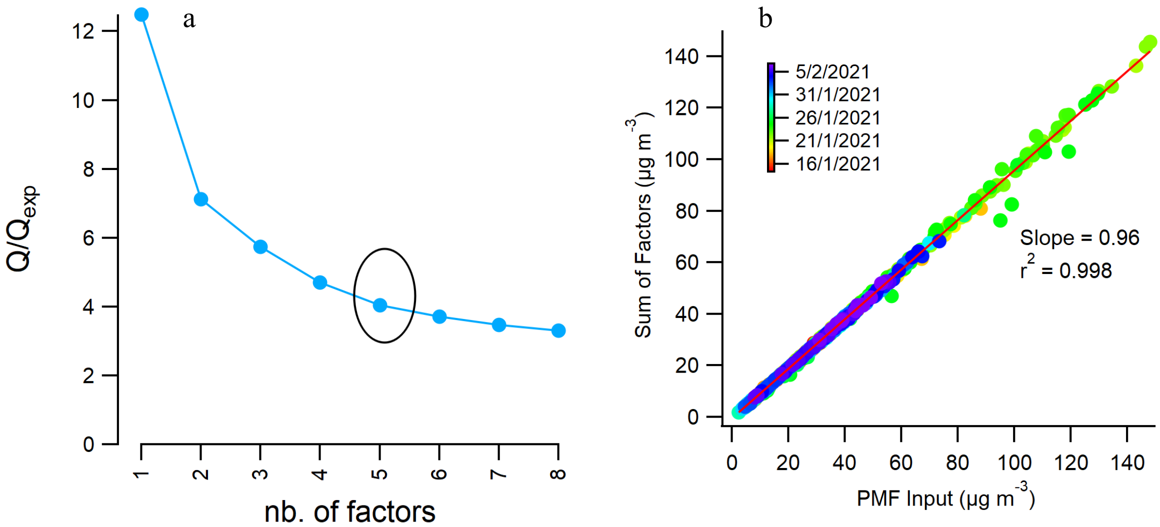

Figure S4. (a) The value of Q/Qexp (Canonaco et al., 2013) as a function of the number of factors (nb. Of factors) with the circle highlighting the number of 5 factors that best represented the current dataset; and (b) scatter plot between the sum of all OA factors (5-factor solution) and the PMF input with the slope and determination of correlation (r^2) being close to unity.

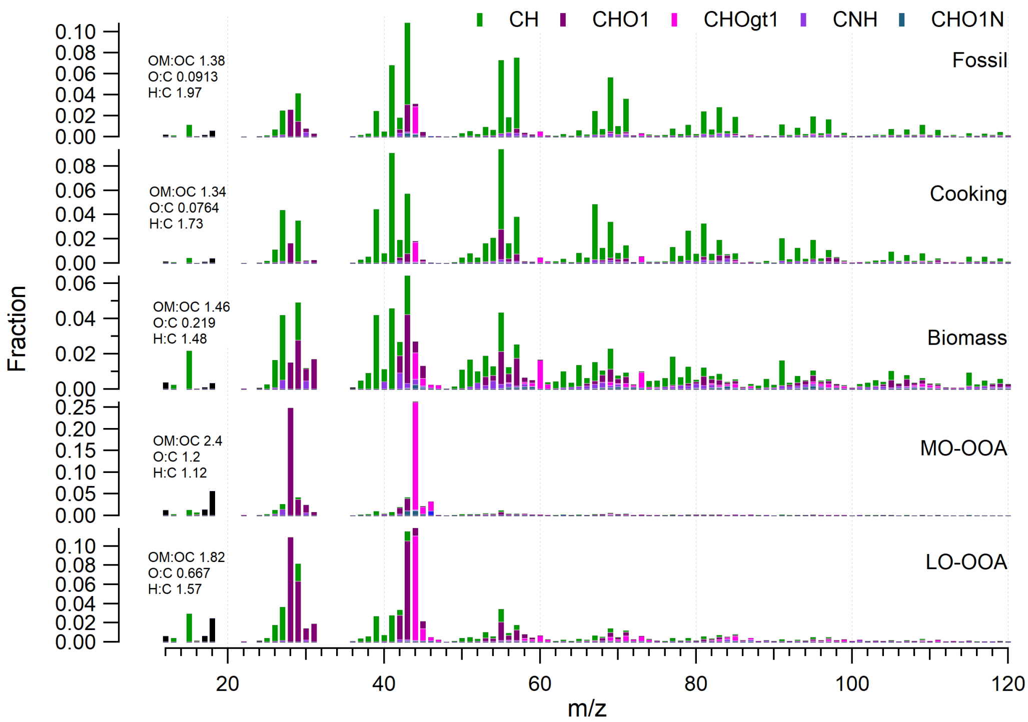

Figure S5. Normalized mass spectra of the OA factors. MO-OOA and LO-OOA were summed up as one OOA in the main text for better comparison across different years. OM:OC, O:C, and H:C ratios are calculated using the improved-ambient (IA) method (Canagaratna et al., 2015).

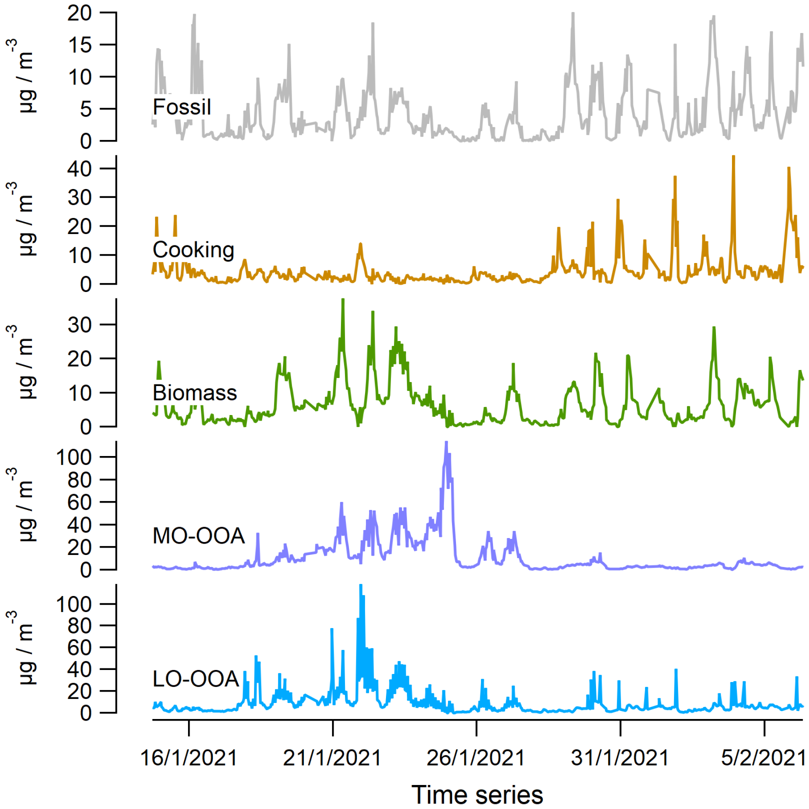

Figure S6. Time series of the OA factors for the 5-factor solution.

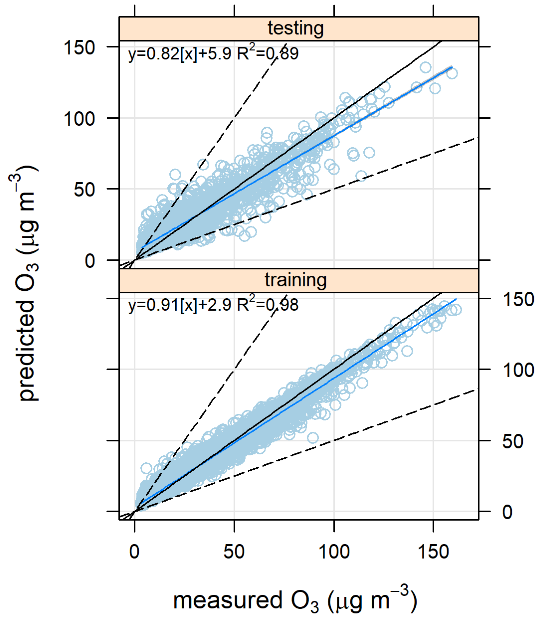

Figure S7. Time series correlation between the predicted and measured O_3 using the random forest model.

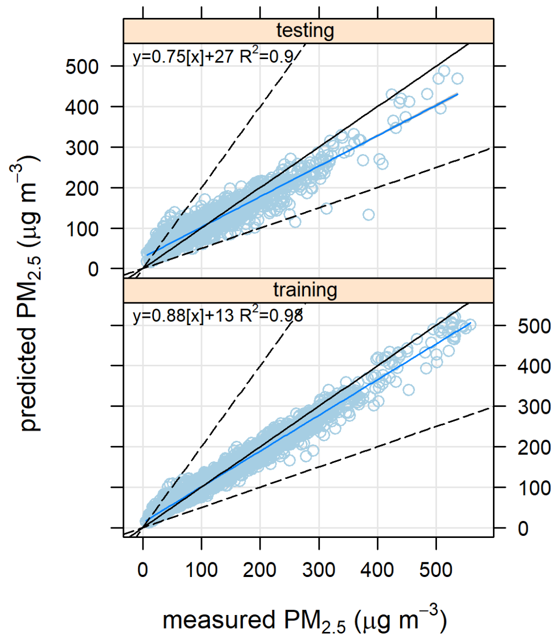

Figure S8. Time series correlation between the predicted and measured $PM_{2.5}$ using the random forest model.

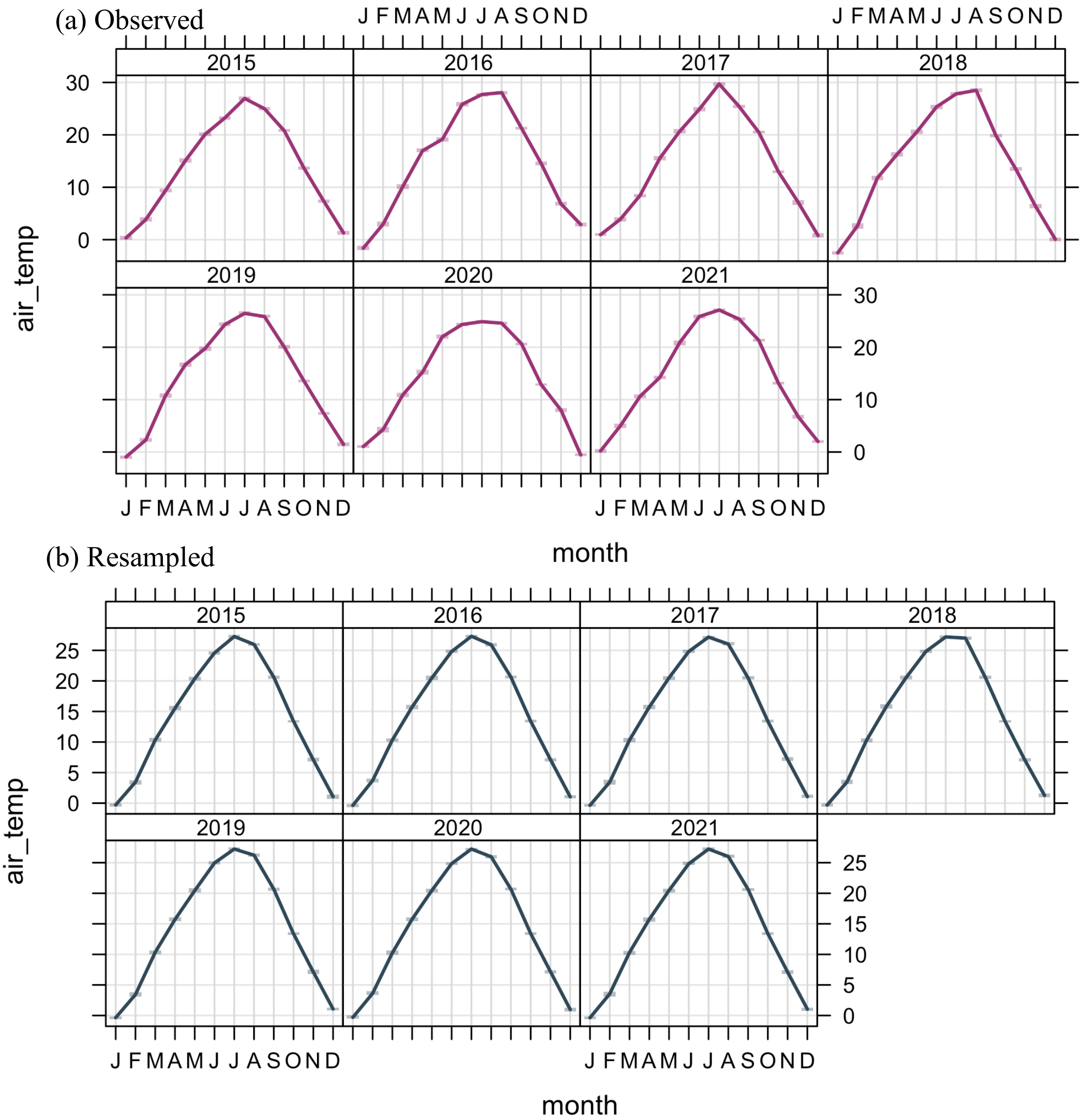

Figure S9. Monthly variation of observed (a) and resampled (b) air temperatures (air_temp in ºC) for 2015-2021. The resampled air temperatures were invariant across the years, in contrast to that for the observed temperatures.

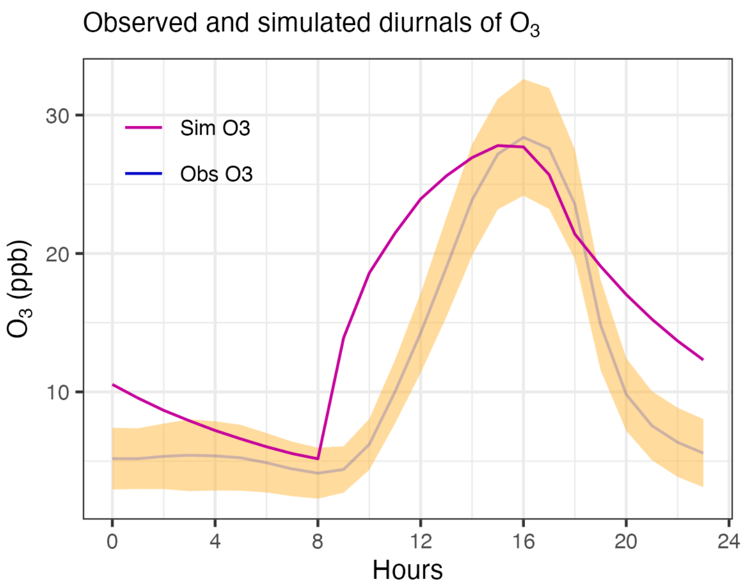

Figure S10. Mean diurnal of the simulated (Sim) and observed O_3 during the sampling period. The shade area represents one standard deviation of the measurement.

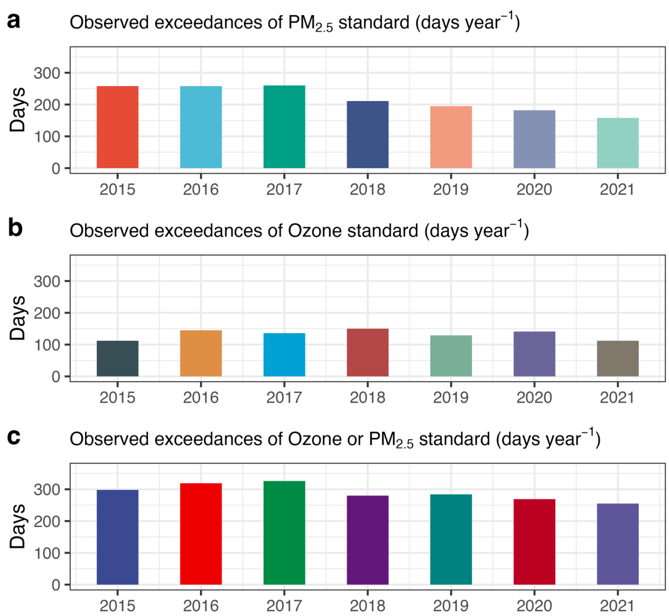

Figure S11. Observed exceedance frequency (in days $year^{-1}$) of Ozone or $PM_{2.5}$ standard (NAAQS level-1) in the biggest city (i.e., Xi'an) in Fenwei Plain from 2015 to 2021. Ozone and $PM_{2.5}$ were averaged from 13 monitoring sites in Xi'an.

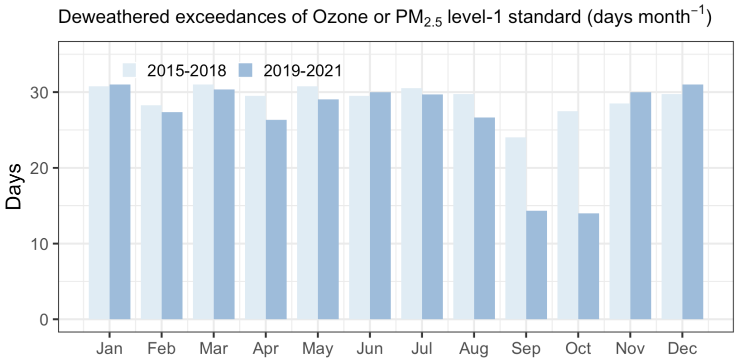

Figure S12. Deweathered exceedances of ozone or $PM_{2.5}$ level-1 standard for 2015-2018 and 2019-2021. Ozone and $PM_{2.5}$ were averaged from 13 monitoring sites in Xi'an with full 2015 to 2021 records.

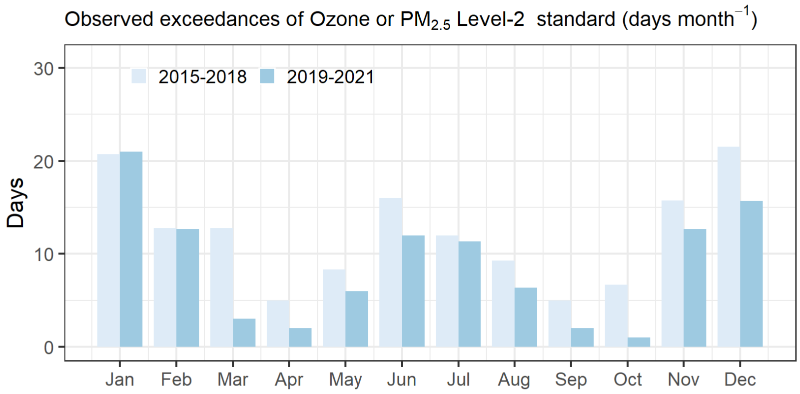

Figure S13. Observed exceedances of ozone or $PM_{2.5}$ level-2 standard for 2015-2018 and 2019-2021. Ozone and $PM_{2.5}$ were averaged from 13 monitoring sites in Xi'an with full 2015 to 2021 records.

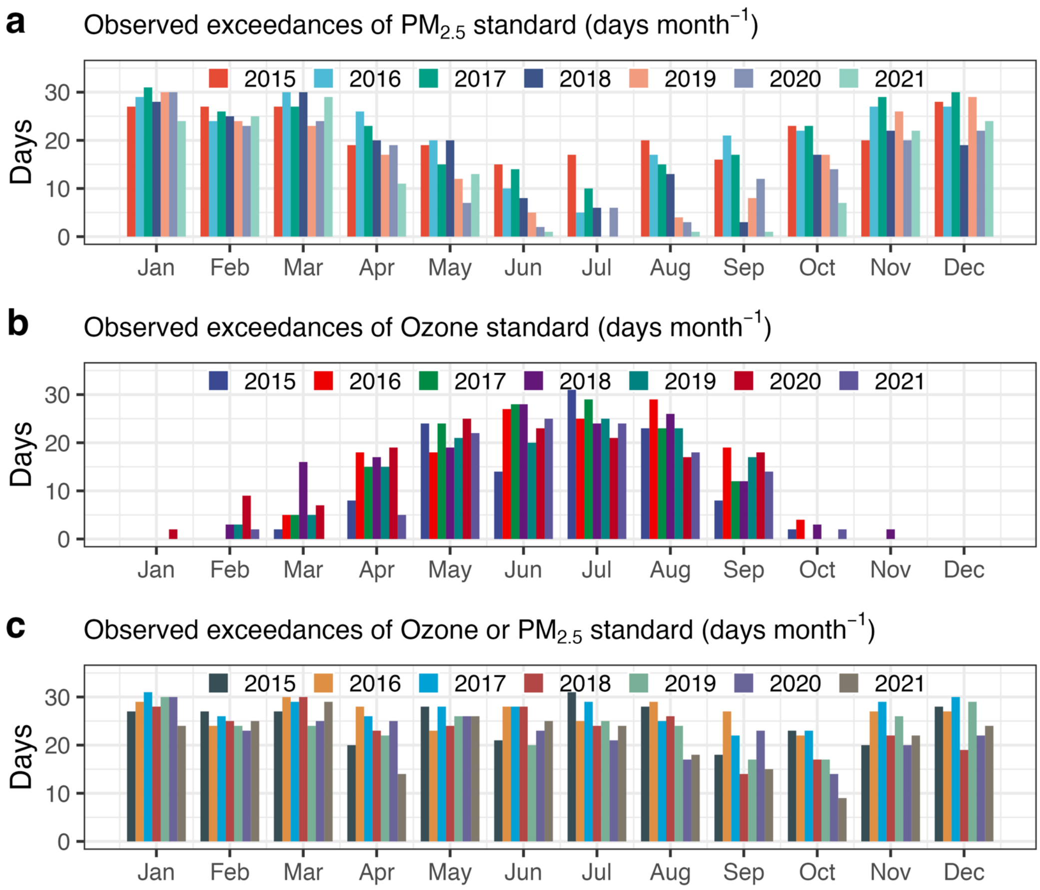

Figure S14. Observed exceedance frequency (in days month^{-1}) of Ozone or $PM_{2.5}$ standard (NAAQS level-1) in the biggest city (i.e., Xi'an) in Fenwei Plain from 2015 to 2021. Ozone and $PM_{2.5}$ were averaged from 13 monitoring sites in Xi'an.

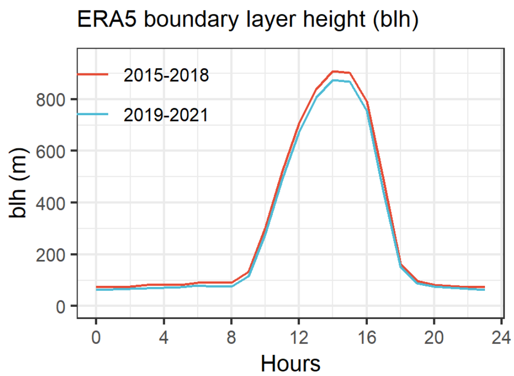

Figure S15. Mean boundary layer height (blh) for 2015-2018 and 2019-2021.

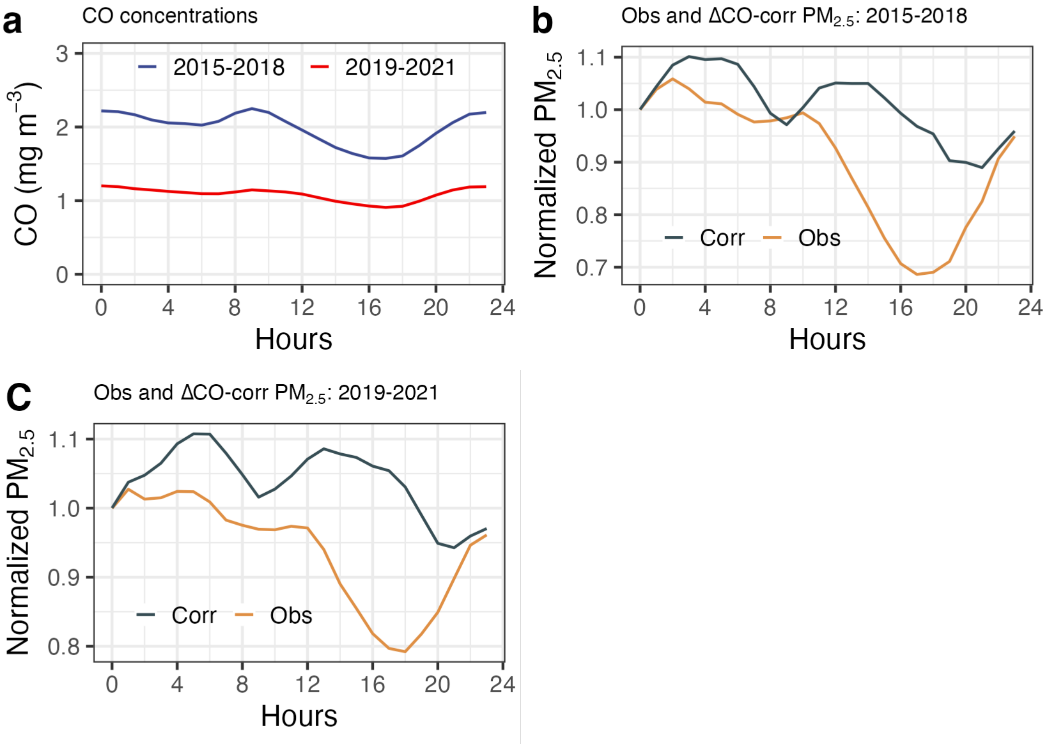

Figure S16. Diurnals of CO (a); observed and ΔCO corrected $PM_{2.5}$ for 2015-2018 (b) and 2019-2021 (c). $PM_{2.5}$ concentrations were normalized to the first hour of the day.

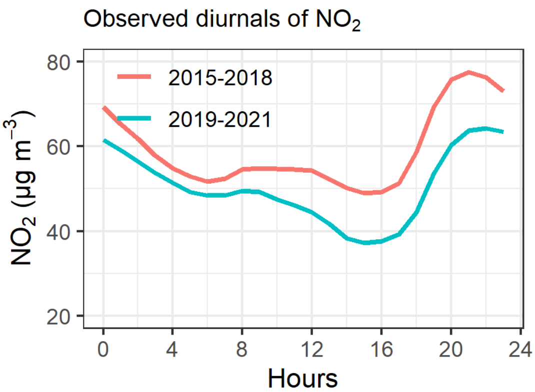

Figure S17. Observed diurnal of NO_2 in January-February for 2015-2018 and 2019-2021.

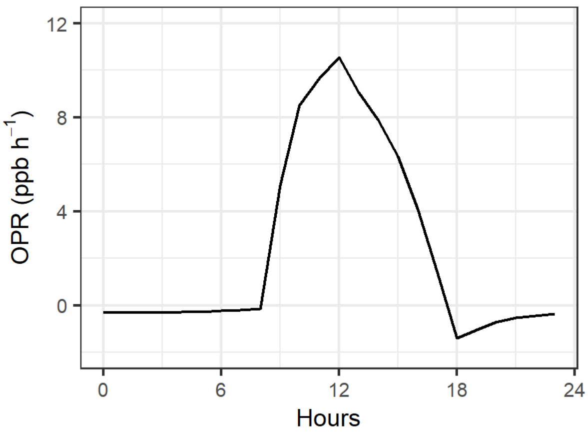

Figure S18. Simulated ozone production rate (OPR at ppb h^{-1}) from 0-D box model.

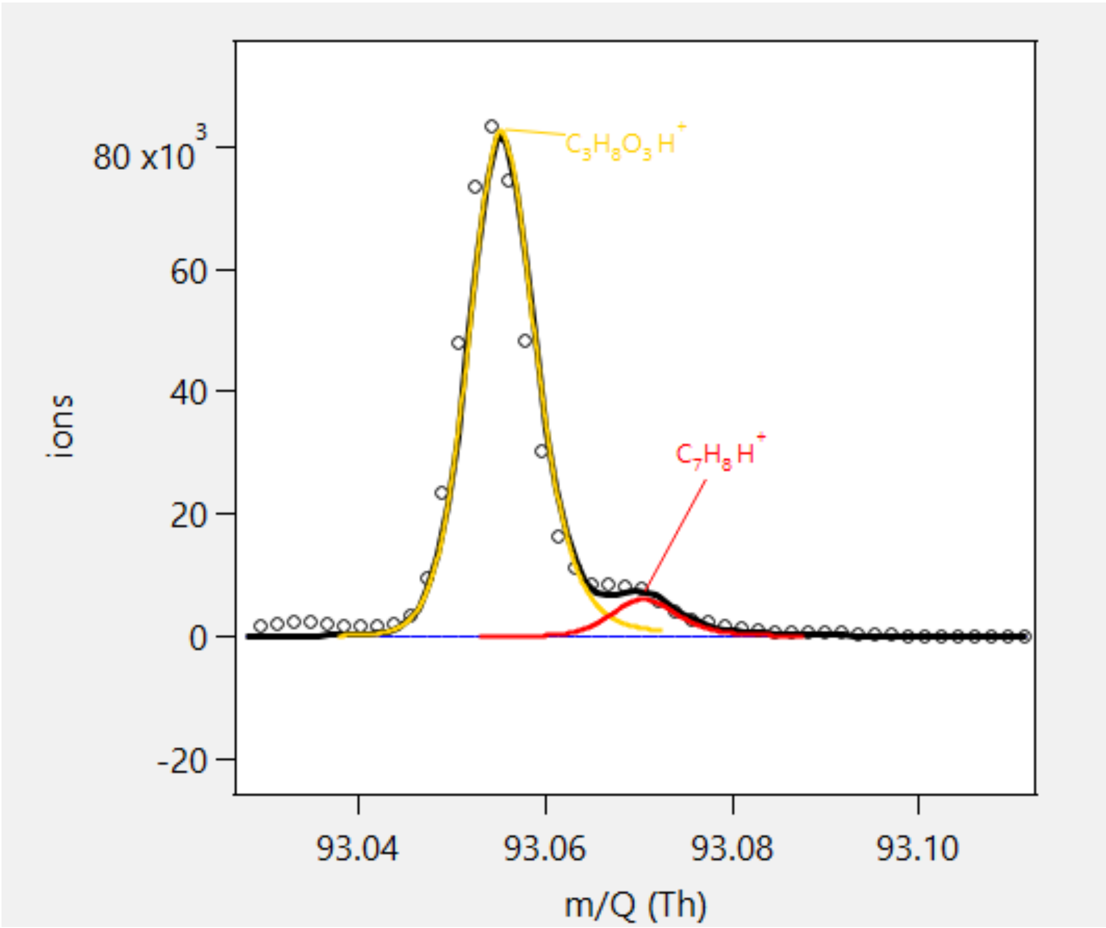

Figure S19. The organic ions at m/z 93. Toluene ion ($C_7H_8H^+$) had a strong neighbor ion, which can be hardly separated by a low-mass resolution mass analyzer.

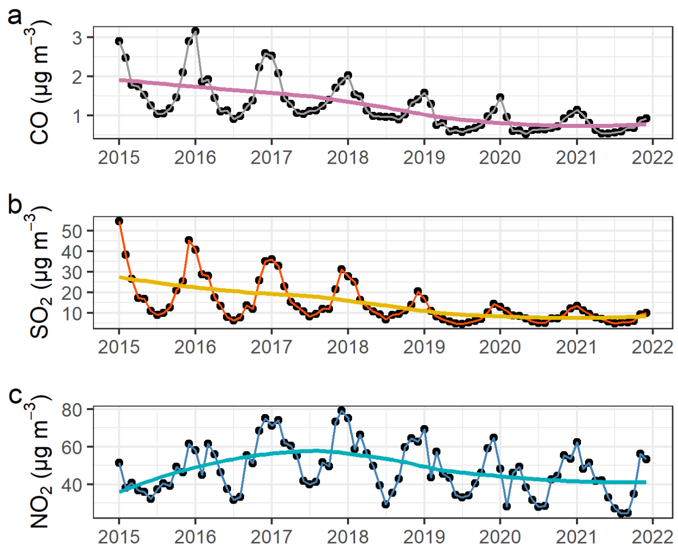

Figure S20. Month means of CO, SO_2, and NO_2 from 2015 to 2022. The smooth line is fitted using a Locally Weighted Least Squares Regression.

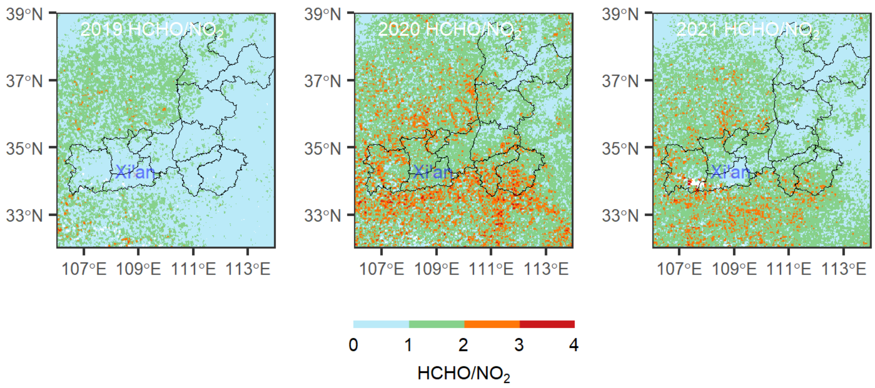

Figure S21. HCHO to NO_2 ratios ($HCHO/NO_2$) measured by the TROPOMI satellite instrument in January-February in 2019, 2020, and 2021.

Table S1. A list of the VOC species, the proton transfer reaction rate coefficients (k_{PTR}) between the hydronium ion (H_3O^+) and selected VOCs, and the obtained sensitivities during calibration.

VOC species	k_{PTR} (10^{-9} molec cm^{-3} s^{-1})	Sensitivity (cps ppbv^{-1})
Benzene	1.93	2,351
Toluene	2.08	2,446
m-Xylene	2.27	3,066
1,2,4-Trimethylbezene (TMB)	2.4	2,835
Acetone	3.44	6,773
Methyl ethyl ketone (MEK)	3.39	5,191
Acetonitrile	4.2	1,481
Acetaldehyde	3.24	1697

Table S2. A list of VOC/OVOC species that were included in the box model.

Formula	Assignment	Mean (ppb)
HCHOH	Formaldehyde[a]	4.16
C3H6OH	acetone	3.39
C4H6O2H	butanedione	1.63
C2H4OH	acetaldehyde	1.20
C6H6H	benzene	1.19
C6H6OH	phenol	0.85
C7H8H	toluene	0.76
C3H6O2H	Methyl acetate	0.35
C4H8OH	Butyraldehyde	0.29
C4H6OH	MEK	0.29
C5H9	Isoprene	0.23
C3H4O2H	Propanal	0.13
C4H6OH	MVK	0.10
C3H4OH	Acrolein	0.10
C9H13	TMB	0.03

Table S3. Sampling time and instruments conducted at the same urban sampling site in Xi'an.

Sampling time	Season	Instrument	References
2012.11.15 – 2013.2.21	2012-2013 winter	PM_1-ACSM	Zhong et al. (2020)
2013.12.13 – 2014.1.6	2013-2014 winter	$PM_{2.5}$-AMS	Elser et al. (2016)
2018.12.4 – 2019.3.15	2018-2019 winter	$PM_{2.5}$-SP-AMS	Duan et al. (2022)
2020.1.18 – 2020.1.31	2019-2020 winter	$PM_{2.5}$-SP-AMS	Duan et al. (2021)
2021.1.14 – 2021.2.6	2020-2021 winter	$PM_{2.5}$-SP-AMS	This study

Table S4. Mean and one standard deviation (sd) chemical composition of non-refractory particulate matter (NR-PM) and the OA factor for the winter in 2012-2014 and 2018-2021. All in μg m^{-3}.

Species	2012-2014	sd (%)	2018-2021	sd (%)
OA	125.4	78.5 (62%)	48.1	6.1 (13%)
Sulfate	52.6	57.7 (110%)	20.3	9.9 (49%)
Nitrate	34.9	30.9 (88%)	17.6	3.0 (17%)
Ammonium	21.0	9.6 (46%)	10.2	2.8 (27%)
Chloride	27.4	30.2 (110%)	4.5	1.8 (40%)
OA factors				
Fossil	37.7	16.4 (44%)	8.8	4.7 (53%)
Biomass	33.5	29.4 (88%)	9.3	2.7 (29%)
Cooking	19.6	12.0 (61%)	3.1	0.7 (22%)
OOA	26.3	20.8 (79%)	23.3	3.2 (14%)

References:

Canagaratna, M. R., Jimenez, J. L., Kroll, J. H., Chen, Q., Kessler, S. H., Massoli, P., Hildebrandt Ruiz, L., Fortner, E., Williams, L. R., Wilson, K. R., Surratt, J. D., Donahue, N. M., Jayne, J. T., and Worsnop, D. R.: Elemental ratio measurements of organic compounds using aerosol mass spectrometry: characterization, improved calibration, and implications, Atmos. Chem. Phys., 15, 253-272, 10.5194/acp-15-253-2015, 2015.

Canonaco, F., Crippa, M., Slowik, J. G., Baltensperger, U., and Prévôt, A. S. H.: SoFi, an IGOR-based interface for the efficient use of the generalized multilinear engine (ME-2) for the source apportionment: ME-2 application to aerosol mass spectrometer data, Atmos. Meas. Tech., 6, 3649-3661, doi:10.5194/amt-6-3649-2013, 2013.

Duan, J., Huang, R.-J., Chang, Y., Zhong, H., Gu, Y., Lin, C., Hoffmann, T., and O'Dowd, C.: Measurement report of the change of PM2.5 composition during the COVID-19 lockdown in urban Xi'an: enhanced secondary formation and oxidation, Science of The Total Environment, 148126, https://doi.org/10.1016/j.scitotenv.2021.148126, 2021.
Duan, J., Huang, R. J., Gu, Y., Lin, C., Zhong, H., Xu, W., Liu, Q., You, Y., Ovadnevaite, J., Ceburnis, D., Hoffmann, T., and O'Dowd, C.: Measurement report: Large contribution of biomass burning and aqueous-phase processes to the wintertime secondary organic aerosol formation in Xi'an, Northwest China, Atmos. Chem. Phys., 22, 10139-10153, 10.5194/acp-22-10139-2022, 2022.
Elser, M., Huang, R. J., Wolf, R., Slowik, J. G., Wang, Q., Canonaco, F., Li, G., Bozzetti, C., Daellenbach, K. R., Huang, Y., Zhang, R., Li, Z., Cao, J., Baltensperger, U., El-Haddad, I., and André, P.: New insights into PM2.5 chemical composition and sources in two major cities in China during extreme haze events using aerosol mass spectrometry, Atmospheric Chemistry and Physics, 16, 3207-3225, 10.5194/acp-16-3207-2016, 2016.
Zhong, H., Huang, R.-J., Duan, J., Lin, C., Gu, Y., Wang, Y., Li, Y., Zheng, Y., Chen, Q., Chen, Y., Dai, W., Ni, H., Chang, Y., Worsnop, D. R., Xu, W., Ovadnevaite, J., Ceburnis, D., and O'Dowd, C. D.: Seasonal variations in the sources of organic aerosol in Xi'an, Northwest China: The importance of biomass burning and secondary formation, Science of The Total Environment, 139666, https://doi.org/10.1016/j.scitotenv.2020.139666, 2020.